Elasto-Plastic Constitutive Models for Stress-Strain Behaviour of Sand

by Hidekazu MURATA*, Noriyuki YASUFUKU* and Hirokuni OKAFUJI**

(Received July 13, 1985)

Abstract

Three constitutive models were investigated based on the concept of a non-associated flow rule. The key concept is the assumption that sand can be regarded as an isotropic work hardening elasto-plastic material. It was proved that the proposed elasto-plastic models, especially Model I could effectively represent the yield and stress-deformation characteristics of sand.

1. Introduction

Sand materials are characterized by the property of producing dilatancy during shear deformation, and the stress-deformation charactristics are remarkably influenced by a stress path and a strain history. Therefore, it is desirable to establish the simple stress-strain relation which can predict the complicated characteristics of sand in regards to such matters as the deformation and stablity analysis of granular soils.

In order to clarify the stress-strain behaviour of granular soils in particle-crushing regions, the authors[1)-3)] have investigated the yielding characterisics of sand in detail using a multi-step stress path method. The following results have been obtained.

(1) The shape of the yield curve of sand in a particle-crushing region is similar to that of the yield curves for clayly soils proposed by Roscoe et al.,[4),5)] rather than that for sand derived by Lade et al.[6)].

(2) The new yield curve and stress-strain equations, derived based on a critical state energy theory, are well conformable with the experimental stress-strain curves in a particle-crushing region.

However, there are some foundmental problems in the case of predicting stress-strain curves of sand under a wide stress range by using the critical state energy theory. It is impossible to apply the concept of the associated flow rule to sand under a non particle-crushing region because sand produces expansion during shear deformation.

Based on the concept of the non-associated flow rule, this paper investigates three constitutive models to predict stress-strain behaviour of sand under a wide stress range. The key concept in this treatment is the assumption that sand can be regarded as an isotropical work hardening elasto-plastic material. The form of the yield function for sand is discussed through the triaxial compression test results of sand in a high stress region. Both plastic potential and hardening function are derived by using the state parameter S_s which is proposed by Moroto[7),8)].

*Department of Construction Engineering

**Graduate student, Department of Construction Engineering

2. Formulation of stress-strain relations

2.1 Stress parameter and strain increment parameter

The following stress and plastic strain increment parameters are used in this study.

$$p = (\sigma_1 + \sigma_2 + \sigma_3) / 3 \tag{1}$$

$$q = {}^1\!/\!\sqrt{2} \cdot \{ (\sigma_1 - \sigma_3)^2 + (\sigma_3 - \sigma_2)^2 + (\sigma_2 - \sigma_1)^2 \}^{1/2} \tag{2}$$

$$\eta = q/p \tag{3}$$

where p is the mean principal stress, q is the deviator stress, η is the stress ratio and σ_1, σ_2 and σ_3 are the principal stresses, respectively.

$$dv^p = d\varepsilon_1^p + d\varepsilon_2^p + d\varepsilon_3^p \tag{4}$$

$$d\varepsilon^p = \sqrt{2} \{ (d\varepsilon_1^p - d\varepsilon_3^p)^2 + (d\varepsilon_3^p - d\varepsilon_2^p)^2 + (d\varepsilon_2^p - d\varepsilon_1^p)^2 \}^{1/2} \tag{5}$$

where dv^p is the plastic volumetric strain increment, $d\varepsilon^p$ is the plastic shear strain increment, and $d\varepsilon_1$, $d\varepsilon_2$ and $d\varepsilon_3$ are the principal plastic strain increment tensors, respectively.

2.2 Derivation of stress-strain relations

In this paper, it is assumed that there exist the plastic potential function g, and the yield function f for sand and that the concept of the non–associated flow rule can be applied. The total strain increment tensor $d\varepsilon_{ij}$ is assumed to be the sum of an elastic strain increment tensor $d\varepsilon_{ij}^e$ and a plastic strain increment tensor $d\varepsilon_{ij}^p$, such that

$$d\varepsilon_{ij} = d\varepsilon_{ij}^e + d\varepsilon_{ij}^p \tag{6}$$

The elastic strain increment tensor is given as,

$$d\varepsilon_{ij}^e = \frac{\kappa}{1+e} \cdot \frac{dp}{p} \cdot \frac{1}{3} \delta_{ij} \tag{7}$$

where e is a void ratio, κ is the slope of the e–ln p swelling curve.

Applying the concept of the non–associated flow rule,[11] the plastic strain increment tensor is formulated by

$$d\varepsilon_{ij}^p = h \cdot \frac{\partial g}{\partial \sigma_{ij}} \cdot df = h \left\{ \frac{\partial g}{\partial p} \frac{\partial p}{\partial \sigma_{ij}} + \frac{\partial g}{\partial q} \frac{\partial q}{\partial \sigma_{ij}} \right\} df \tag{8}$$

where, h is the hardening function, which is the scalar function of the stress and strain history, g is the plastic potential function, f is the yield function and σ_{ij} is the stress tensor. Here, the yielding condition is given by the following equation.

$$f - f^* = 0 \tag{9}$$

where f^* is the highest value of f encountered in the loading program. If the yield, plastic potential and hardening functions are formulated as the function of the stress parameters, the stress-strain relations can be derived by using Eqs. (6), (7) and (8) definetely.

2.3 Properties of the yield and plastic potential functions

Poorooshasb[10] proposed the following yield function by investigating the yield characteristics of sand under a relatively low stress range in detail.

$$f = \eta + m \cdot \ln p \tag{10}$$

where m is the constant determind experimentally.
The value of coefficient m was found to be equal to 0.6 for the sand used in his study. Fig. 1 shows the normalized yield curve in the p/p_0-q/p_0 diagram depicted using Eq. (10),

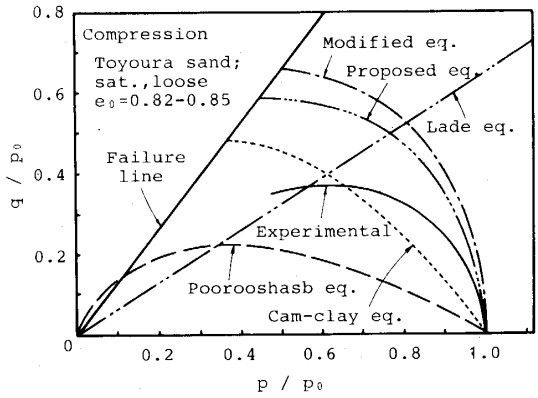

Fig. 1 Comparison of the predicted and experimental yield curves.

together with the yield curve indicated by Miura et al. [1),12)] experimentally. where p_0 is the value of p at $\eta = 0$. In Fig. 1, other four yield curves proposed by Roscoe et al., [4),5)] Lade et al.,[6)] and the authors[2)] are depicted. This figure indicates that the yield curves showed experimentally by the authors is not only different from the yield curve based on Eq. (10) but also different from ones proposed by another reaserchers. Therefore, in order to obtain a more conformable equation that agrees with the experimental yield curves in a wide stress region, the authors searched for a better expression for the yield function f. After all, the authors found the following expression to give an excellent result.

$$f = \eta^2 + m \cdot \ln p \tag{11}$$

where m is the parameter depended on the stress states. The method to determine the parameter m will be discussed in section 3.1. Here, Model I is derived based on Eq. (11), and Model II and Model III are derived based on Eq. (10).

The plastic potential function g, from which the gradient of the plastic strain increment may be obtained, is derived by using the state parameter S_s proposed by Moroto et al.[7),8)]. The equation for the plastic energy dissipation per unit volume dw^p is expressed as follows.

$$dW^p = \sigma_{ij}\, d\varepsilon_{ij}^p = pdv^p + qd\varepsilon^p \tag{12}$$

Moroto[7),8)] pointed out that the normalized dissipated shear work dS_s indicated by the following equation can be a state parameter of granular soils.

$$dS_s = \frac{dW_s^p}{p} \tag{13}$$

Combining Eqs. (12) and (13), the normalized dissipated shear work is given by

$$dS_s = dv^p + \eta \cdot d\varepsilon^p \tag{14}$$

where, dW_s^p is the increment of plastic work done due to shear and dv^p is the plastic volumetric increment strain due to dilatancy. Fig. 2 shows typical plots of S_s as the function of the shear strain for Toyoura sand. Let the gradient of the curve S_s and ε be denoted by α. This figure indicats that the parameter α is approximately constant regardless of the magnitude of the shear strain and stress path. As it might be assumed that the elastic shear strain ε^e can be ignored, Fig. 2 gives the following equation

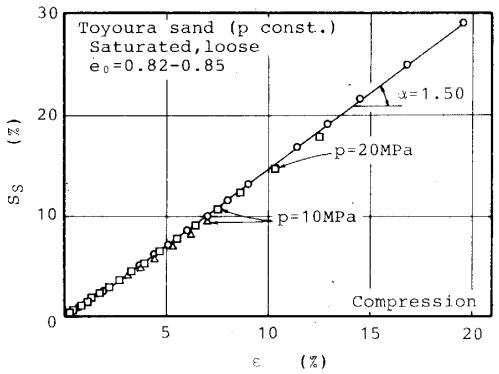

Fig. 2 Relationship between state parameter S_s and shear strain ε obtained by constant p test

$$S_s = \int \frac{dW_s^p}{p} = \int \alpha \cdot d\varepsilon^p \tag{15}$$

Total differential form of Eq. (15) is expressed as

$$dS_s = \alpha \cdot d\varepsilon^p \tag{16}$$

Combinding Eqs. (14) and (16), the plastic strain increment vector due to shear is given by

$$\frac{dv^p}{d\varepsilon^p} = \alpha - \eta \tag{17}$$

where, parameter α is a constant which evaluate stress-dilatancy characteristics during the consolidation and the shear deformation, and is value of η at $dv^p/d\varepsilon^p = 0$. Fig. 3 shows the relation between η and $dv^p/d\varepsilon^p$ for Toyoura sand under constant p and constant σ_3 conditions, compared with the predicted line by Eq. (17). It is seen from this figure that the calculated line by Eq. (17) agrees very well with the experimental results and that the relation between $dv^p/d\varepsilon^p$ and η may be determined uniquely independent of stress path. From this experimental result it can be said Eq. (17) has a comformability regardless of the stress paths. Then, combining Eq. (17) and the concept of the normality rule, the plastic potential function is derived as follows.

$$g = \eta + \alpha \cdot \ln p \tag{18}$$

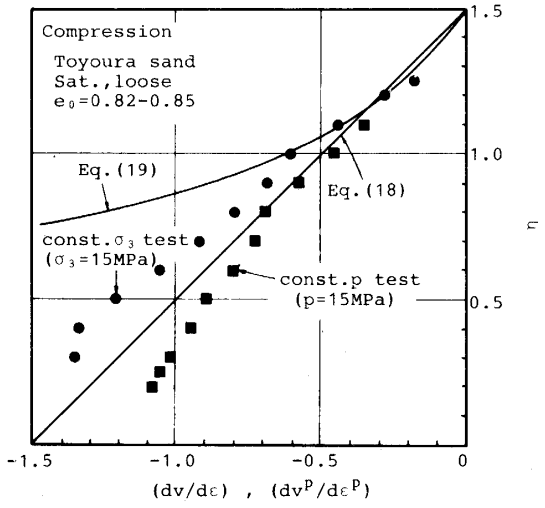

Fig. 3 Prediction of stress-dilatancy characteristics

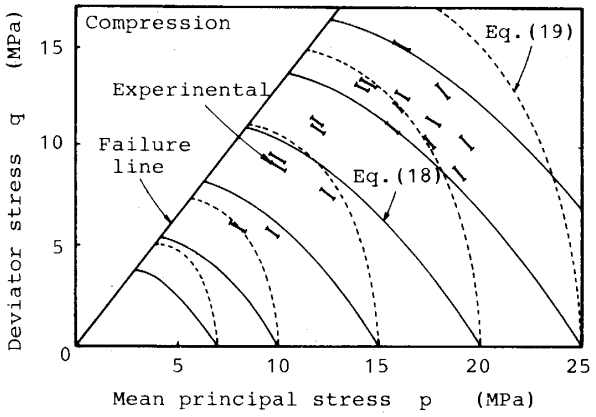

Fig. 4 Family of the plastic potential curves in p-q space

Fig. 4 shows the family of the plastic potential curve depicted in the p-q diagram using Eq. (18), together with the plastic potential segments obtained in the particle crushing region experimentally. This figure indicates that the plastic potential curves based on Eq. (18) apporoximately agree with the plastic potential segments observed, therefore, Eq. (18) may be the reasonable plastic potential function for sand. Eq. (18) is used to derive the elasto-plastic constitutive models called Model I and Model II in this study. Eq. (19) is the another plastic potential function for Model III

$$g = p\left(\frac{\alpha^2 + \eta^2}{\alpha^2}\right) \tag{19}$$

This plastic potential function is the same type as Burland[9] proposed. The plastic potential function g and the yield function f are summarized in Table 1.

Table 1 The characteristics of three proposed models

	Model I	Model II	Model III
Yield function f	$f = \eta^2 + m \cdot \ln p$	$f = \eta + m \cdot \ln p$	$f = \eta + m \cdot \ln p$
Plastic potential function g	$g = \eta + \alpha \cdot \ln p$	$g = \eta + \alpha \cdot \ln p$	$g = p\left(\frac{\alpha^2 + \eta^2}{\alpha^2}\right)$
Parameter m	$\frac{(\lambda - \kappa)\eta_f^2}{(1+e)a}$	$\frac{(\lambda - \kappa)\eta_f}{(1+e)a}$	$\frac{\lambda - \kappa}{1+e}\frac{\eta_f^2}{a\alpha}$

3. Predication of the stress-strain relations

3.1 Hardening function for Model I

To simplify the disscusion on the hardening function, sand is assumed to be an isotropic hardening material. The state parameter S_s is introduced to determine the hardening function concretely. Fig. 5 shows the relation between $(\eta / \eta_f)^2$ and S_s. From this results, it can be considered that the relation between $(\eta / \eta_f)^2$ and S_s is represented by a unique hyperbolic curve, irrespective of the magunitude of p such that,

$$\frac{\eta}{\eta_f} = \sqrt{\frac{S_s}{a + b \cdot S_s}} \tag{20}$$

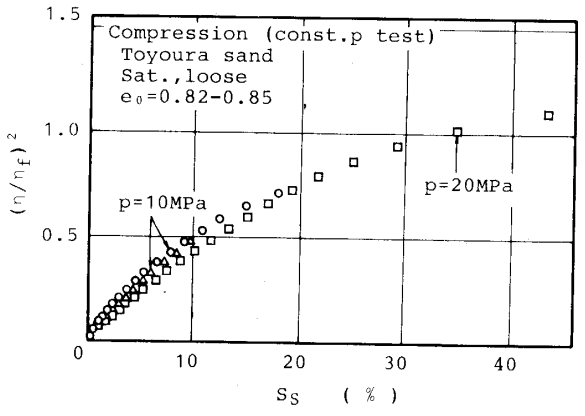

Fig. 5 Relation between S_s and $(\eta / \eta_f)^2$

where, η_f is the stress ratio at failure, which is assumed to be a function of p, a and b are constants. Substitution of Eq. (16) into Eq. (20) gives

$$\frac{\eta}{\eta_f} = \sqrt{\frac{\alpha \cdot \varepsilon^p}{a + \alpha \cdot b \cdot \varepsilon^p}} \tag{21}$$

Differentiating Eq. (21), $d\varepsilon^p$ is given by

$$d\varepsilon^p = \frac{2 \cdot a \cdot \eta \cdot \eta_f^2}{\alpha (\eta_f^2 - b \cdot \eta^2)^2} d\eta \tag{22}$$

Now, for the drained triaxial test at constant p, the plastic shear strain increment is derived from Eqs. (8), (9) and (18) as

$$d\varepsilon^p = h \cdot \frac{1}{p} \cdot 2\eta \cdot d\eta \tag{23}$$

Equating Eps. (22) and (23), the hardening function h is obtained

$$h = \frac{a \cdot \eta_f^2}{\alpha (\eta_f^2 - b \cdot \eta^2)^2} p \tag{24}$$

Therefore, the plastic strain increment tensor $d\varepsilon_{ij}^p$ is given by substituting Eqs. (11), (18) and (24) into Eq. (8). The plastic volumetric strain increment dv^p and the plastic shear strain increment $d\varepsilon^p$ are given as follows, respectively.

$$dv^p = h \frac{\partial g}{\partial p} df = \frac{a \cdot \eta_f^2}{\alpha (\eta_f^2 - b \cdot \eta^2)^2} (\alpha - \eta) \langle 2\eta \cdot d\eta + m \frac{dp}{p} \rangle \tag{25}$$

$$d\varepsilon^p = h \frac{\partial g}{\partial q} df = \frac{a \cdot \eta_f^2}{\alpha (\eta_f^2 - b \cdot \eta^2)^2} \langle 2\eta \cdot d\eta + m \frac{dp}{p} \rangle \tag{26}$$

Here, the hardening functions for Model II and Model III are also determined by the above same manner. These results are sammarized in Table 1.

3.2 Determination of soil parameters

Eq. (25) gives the plastic strain increment dv^p under isotropic consolidated condition as

$$dv^p = \frac{a}{\eta_f^2} \cdot m \cdot \frac{dp}{p} \tag{27}$$

On the other hand, the isotropic consolidation components of the plastic volumetric strain increment dv^p is formulated based on the e–ln p curve.

$$dv^p = \frac{\lambda - \kappa}{1 + e} \frac{dp}{p} \tag{28}$$

Equating Eqs. (26) and (27), the parameter m is given by

$$m = \frac{(\lambda - \kappa)\,\eta_f^2}{(1 + e)\,a} \tag{29}$$

where λ and κ are parameters depending on the stress state. Substituting Eq. (29) into Eq. (11), Eq. (11) gives

$$f = \eta^2 + \frac{(\lambda - \kappa)\,\eta_f^2}{(1 + e)\,a} \ln p \tag{30}$$

From Eq. (30), it is known that the shape of its predicted yield curve changes by the stress state. The parameter m for Model II and III obtained by the above manner is shown in Table 1.

Fig. 6 shows the isotropic compression and swelling test results for Toyoura sand under the cell pressures up to 50 MPa. From Fig. 6, it can be seen that the e–ln p curve becomes bilinear. Fig. 7 indicates the λ –ln p characteristics, showing that the value of λ is dependent on the magnitude of p, and κ is a constant independent of p.Based on λ –ln p relationship of Fig. 7, the parameter λ is formulated as follows.

$$\begin{aligned} \lambda &= \lambda_1 + d_1 \cdot \ln p \qquad (p < p_y) \\ &= \lambda_1 + (d_1 - d_2) \cdot \ln p_y + d_2 \cdot \ln p \qquad (p_y < p < p_{cs}) \end{aligned} \tag{31}$$

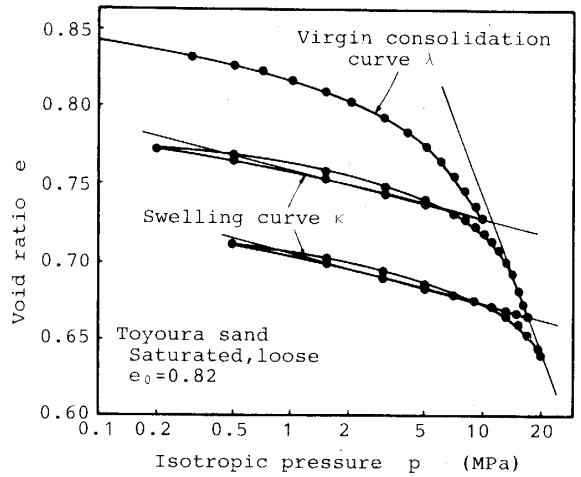

Fig. 6 Relation between void ratio e and isotropic pressure p

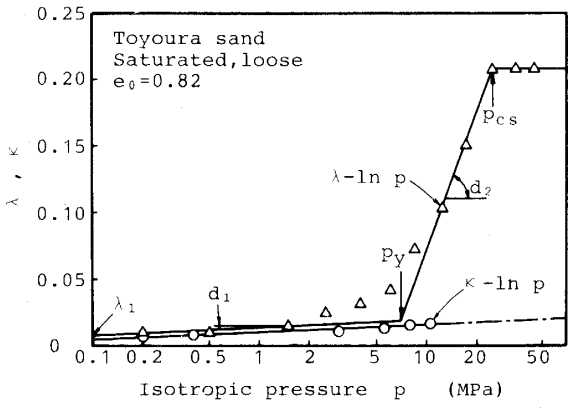

Fig. 7 Relation between λ, κ and isotropic pressure p

where, λ_1 is the value of λ at p = 0.98 MPa, p_y is the consolidated yield stress, p_{cs} is the value of p at λ =constant, and d_1 and d_2 are slopes of λ −ln p curves. Fig. 8 shows the relation between η_f and p at failure, using the triaxial compression test results under a wide stress range.

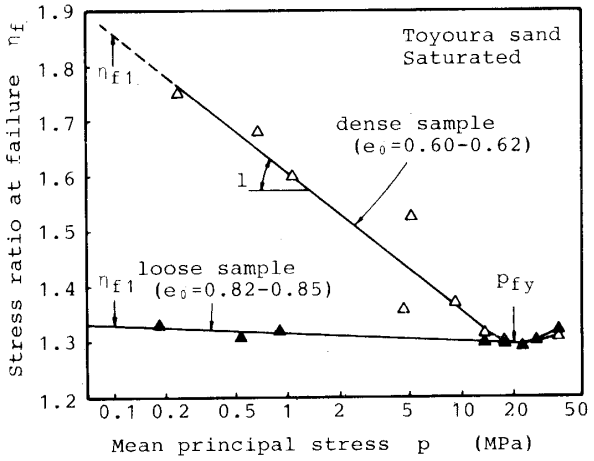

Fig. 8 Relation between stress ratio at failure η_f and mean principal stress p at failure

It is seen from this figure that the strengh parameter η_f is dependent on the value of p, therefore, we assumed that η_f is formulated as follows.

$$\eta_f = \eta_{f1} - l \cdot \ln p \qquad (p < p_{fy})$$
$$= \eta_{f1} - l \cdot \ln p_{fy} \qquad (p > p_{fy}) \tag{32}$$

where, η_{f1} is the value of η at p = 0.98 MPa and p_{fy} is the value of p at η_f = const. All of the soil parameters for Toyoura sand obtained by the above-mentioned method are sammarized in Table 2.

Table 2 Soil parameters for Toyoura sand

Parameter	a	b	α	λ_1	κ	η_{f1}	l	d_1	d_2
Model Ⅰ. Ⅲ	0.152	0.553	1.50	0.007	0.004	1.33	0.006	0.003	0.1480
Model Ⅱ	0.070	0.813	1.50	0.007	0.004	1.33	0.006	0.003	0.1480

3.3 Verification of constitutive models

The predicted yield curves for Toyoura sand by Model I,II and III are depicted in Fig. 9. The yield curve predicted by Model I is well comparable with the experimental yield curve investigated in a particle-crushing region rather than those by Model II and III.

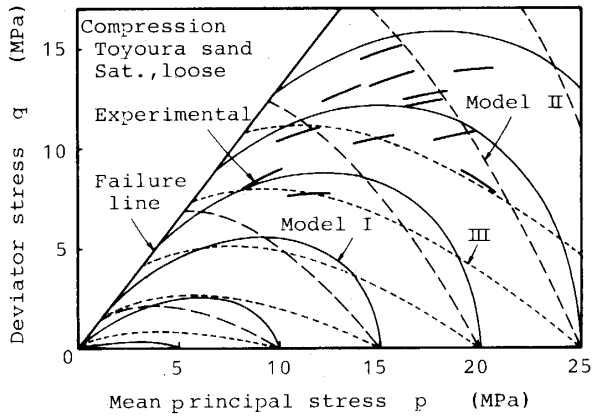

Fig. 9 Comparison of the predicted and experimental yield curves

Fig. 10 shows the yield curve predicted by the yield function (Ep. (11)) of Model I in q/p_0–p/p_0 space. This figure indicates the interesting results that the shape of predicted yield curve depends on the value of p. Fig. 11 shows the stress–strain curves of the drained triaxial compression test under a constant confining pressure, and the predicted stress–strain behaviour of sand excellently.

In order to evaluate the abilities of the proposed models under a wide stress region, We are now investigating the yield characteristics and stress–strain behaviour of sand under a low stress region.

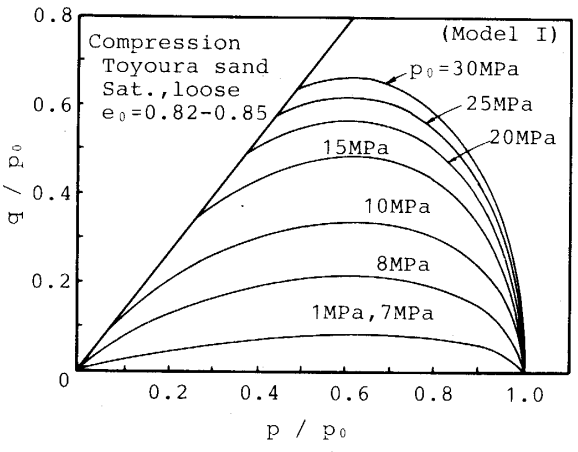

Fig. 10 Effect of the value of p_0 on the shape of normalized yield curve (Model I)

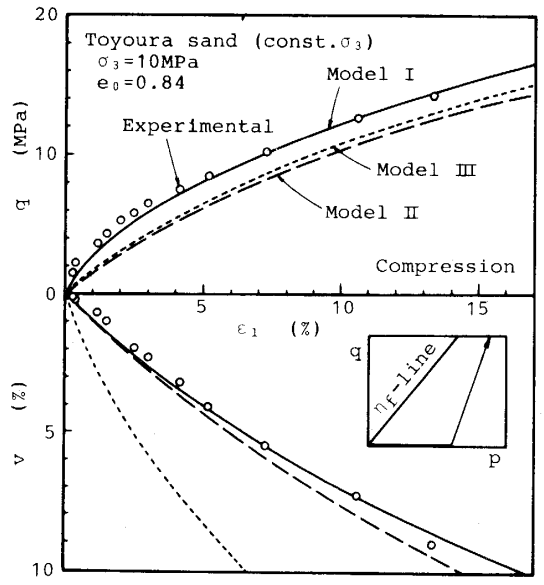

Fig. 11 Prediction of stress–strain curve for standerd triaxial test (constant σ_3)

Conclusions

On the basis of the concept of the non-associated flow rule, three elasto-plastic constitutive models of sand were derived in order to predict the mechanical behaviour of sand under a wide stress region. The following main conclusions were obtained.

1) The yield curve depicted by the Model I proposed is well comparable with the experimental yield curve in a high stress region.
2) The proposed plastic potential function is conformable to the experimental plastic potential curves obtained in a high stress region.
3) The proposed stress-strain relation, especially Model I can satisfactorily predict the experimental stress-strain curves of sand in a high stress region.

Acknowledgement

The authors wish to express their sincere gratitude to Professor N. Miura of Saga University for his kind advice throughout this work.

References

1) Miura, N, Yasufuku, N. and Yamamoto, T., "Yielding characteristics of sand under triaxial compression and extension stresses", Tech. Reps. of the Yamaguchi Univ. Vol. 3, No. 1, pp. 33-45 (1982)
2) Miura, N., Murata, H. and Yasufuku, N., "Stress-strain prediction by a revised Model of Cam-clay", Proc. of Disscussion Session 1A of 11th ICSMFE, San Francisco pp. 144-147 (1985)
3) Miura, N., Murata, H. and Yasufuku, N., "Stress-strain characteristics of sand in a particle-crushing region", Soils and Foundations, Vol. 24, No. 1, pp. 77-89 (1984)
4) Roscoe, K. H., Schofield, A. N. and Thurirajah, A., "Yielding of clay in state wetter than critical", Geotechnique, Vol. 13, No. 3, pp. 211-240 (1963)
5) Roscoe, K. H. and Burland, J. B., "On the generalized stress strain behaviour of "wet clay", Engineering Plasticity, Cambridge Univ. Press., pp. 535-690 (1968)
6) Lade, P. V. and Duncan, J. M., "Elasto-plastic stress-strain theory for cohesionless soil", J. Geotech Eng. Div., ASCE, Vol. 101, No. GT10, pp. 1037-1053 (1975)
7) Moroto, N. and Kawakami, F., "State function of sand deformation", Proc. JSCE, No. 229, pp. 77-86 (1974)
8) Moroto, N., "A new parameter to measure degree of shear deformation of granular material in triaxial compression tests", Soils and Fundations, Vol. 16, No. 4, pp. 1-9 (1976)
9) Burland, J. B., "The yielding and dilation of clay", Correspondence, Geotechnique, Vol. 15, No. 2, pp. 211-214 (1965)
10) Poorooshasb, H. B., "Deformation of sand in triaxial compression", Proc. 4th Asian Regional Conf. on Soil Mech. and Found. Eng., Bangkok, Vol. 1, pp. 63-66 (1978)
11) Hill, R., The Mathematical Theory of plasticity, Oxford Univ. Press London (1950)
12) Miura, N. and Yamamoto, N., "On the yield curve of sand in a paticle-crushing region", Proc. JSCE, No. 326, pp. 83-90 (1982)